Tapered Undulator for SASE FELs

William M. Fawley

Lawrence Berkeley National Laboratory, Berkeley, CA 94720, USA

Zhirong Huang [1], Kwang-Je Kim

Advanced Photon Source, Argonne National Laboratory, Argonne, IL 60439, USA

Nikolai A. Vinokurov

Budker Institute of Nuclear Physics, 11 Ac. Lavrentyev Prosp., 630090, Novosibirsk, Russia

Abstract

We discuss the use of tapered undulators to enhance the performance of free-electron lasers (FELs) based upon self-amplified spontaneous emission (SASE), where the radiation tends to have a relatively broad bandwidth, limited temporal phase coherence, and large amplitude fluctuations. Using the polychromatic FEL simulation code GINGER, we numerically demonstrate the effectiveness of a tapered undulator for parameters corresponding to the existing Argonne low-energy undulator test line (LEUTL) FEL. We also study possible tapering options for proposed x-ray FELs such as the Linac Coherent Light Source (LCLS).

Key words: free-electron laser, tapered undulator, self-amplified spontaneous emission
PACS: 41.60.Cr

1 Introduction

A self-amplified spontaneous emission (SASE) free-electron laser (FEL) is capable of generating extremely high-brightness radiation down to the hard x-ray

[1] Corresponding author. Tel: (630)252-6023; Fax: (630)252-5703; Email: zrh@aps.anl.gov

wavelengths. However, the energy efficiency is quite low for such a device. For a uniform parameter undulator, the FEL efficiency (the ratio of the radiation power to the electron beam power) at saturation is roughly given by the FEL scaling parameter ρ [1], where ρ is typically on the order of 10^{-3} in the x-ray wavelengths.

In order to extract significant radiation power beyond the nominal saturation level, the undulator strength parameter, in principle, can be tapered to maintain the resonant condition as the electron beam loses energy [2]. In this paper, we study the effects of tapered undulators for SASE FELs, with the goal of enhancing the FEL performance and the energy efficiency. We divide our discussions between the exponential growth regime and the saturation regime in the following two sections.

2 Exponential Growth Regime

A free-electron laser uses the resonant condition that guarantees the sustained interaction between the electron beam and the radiation wave. For a planar undulator with undulator period λ_u and undulator strength parameter K, the fundamental resonant wavelength is

$$\lambda_r = \frac{\lambda_u}{2\gamma_0^2}\left(1+\frac{K^2}{2}\right), \tag{1}$$

where $\gamma_0 mc^2$ is the initial electron energy. In the exponential growth regime before saturation, the fractional energy loss of the electron beam due to the FEL interaction is much smaller than ρ. Thus, one can neglect the energy exchange in this regime and use a uniform parameter undulator ($K(z) =$ constant) to maintain the resonant condition. However, additional energy loss due to the emission of wideband spontaneous radiation (including higher harmon-

ics for $K > 1$) in a long undulator beam line can be significant and may even dominate in proposed x-ray FELs, such as the Linac Coherent Light Source (LCLS) [3]. In this case, the beam energy decreases linearly with the undulator distance z, and the undulator parameter K should be tapered accordingly to maintain the resonant condition in order to both not degrade the gain and maintain minimal SASE bandwidth.

Many real undulator beam lines consist of sections separated by short drift spaces (where $K = 0$) used for electron beam steering and diagnostic stations [4]. Therefore the filling factor κ (the ratio of the length occupied by undulator sections to the total undulator line length) should be taken into account. When the power gain length is more than the length of the undulator section (as will probably be true for the LCLS), one can average the FEL interaction over the magnetic structure period. Using, for example, Xie's parametrization [5], one can obtain the effective power gain length [6]

$$L_G = \frac{1}{\kappa^{2/3}\kappa_1^{1/3}} L_{1d}\left[1 + \eta\left(\frac{4\pi L_{1d}}{\lambda_u}\frac{\kappa_1^{2/3}}{\kappa^{2/3}}\frac{\sigma_\gamma}{\gamma_0}, \frac{L_{1d}}{\beta\kappa^{2/3}\kappa_1^{1/3}}\frac{4\pi\varepsilon}{\lambda_r}, \frac{\lambda_r L_{1d}}{4\pi\varepsilon\beta\kappa^{2/3}\kappa_1^{1/3}}\right)\right], \tag{2}$$

where $L_{1d} = \lambda_u/(4\pi\sqrt{3}\rho)$ is the one-dimensional gain length, η is the gain degradation factor defined in Ref. [5], $\sigma_\gamma mc^2$, ε and β are the e-beam energy spread, emittance and average beta function, respectively, and

$$\kappa_1 = \kappa + \frac{1-\kappa}{1 + K^2/2}$$

describes the effect of the drift spaces upon the average longitudinal velocity. In the opposite limit, when each undulator section is longer than two gain lengths (as is true in the Argonne low-energy undulator test line (LEUTL) FEL [7]), we can neglect the gain degradation of the drift spaces if the radiation phase

shift in them has be properly taken into account [8].

3 Saturation Regime

Once the fractional energy loss of the e-beam becomes comparable to the FEL parameter ρ, most electrons fall out of the resonant bandwidth of the radiation, leading to FEL saturation. Nevertheless, as shown by Kroll, Morton and Rosenbluth (referred as KMR hereafter) [2], one can then taper the undulator parameter K to satisfy the resonant condition in the saturation regime to extract additional energy from the electron beam. Previous experiments at microwave frequencies have demonstrated that tapering an undulator substantially increases the output power and extraction efficiency of a single-pass FEL amplifier [9]. In this section, we apply the KMR formalism to study and design tapered undulators for SASE FELs and use the time-dependent FEL code GINGER [10] to demonstrate the effectiveness of tapered undulators for beam parameters that correspond to the LEUTL FEL and the LCLS.

3.1 KMR Formalism

In a tapered undulator, the resonant energy $\gamma_r mc^2$ is defined via

$$\frac{1+K(z)^2/2}{2\gamma_r(z)^2} = \frac{\lambda_r}{\lambda_u} = \text{constant}. \tag{3}$$

In the absence of betatron motion, an electron's equation of motion is

$$\frac{d\theta}{dz} = \frac{4\pi}{\lambda_u}\eta, \quad \frac{d\eta}{dz} = -\frac{1}{\gamma_0}\frac{d\gamma_r}{dz} - \frac{eK[\mathrm{JJ}]}{2\gamma_0^2 mc^2}E\sin(\theta+\phi), \tag{4}$$

where θ is the electron phase relative to a plane wave, $\eta = (\gamma - \gamma_r)/\gamma_0$ is the relative energy deviation, E and ϕ are the slowly varying amplitude and

phase of the radiation field, respectively, and [JJ] is the usual Bessel factor for a planar undulator.

Following KMR [2], a synchronous phase ψ_r is defined through

$$-\frac{1}{\gamma_0}\frac{d\gamma_r}{dz} \equiv \frac{eK[\mathrm{JJ}]}{2\gamma_0^2 mc^2} E \sin\psi_r. \tag{5}$$

In view of Eq. (4), a "synchronous" electron with ponderomotive phase $\psi \equiv (\theta + \phi)$ equal to the synchronous phase ψ_r will maintain its resonant energy $\gamma_r mc^2$ throughout the undulator. Electrons with small energy deviation η perform synchrotron oscillations around the synchronous electron, just as in a rf bucket. Thus, if E and ϕ change adiabatically with z and $\sin\psi_r > 0$, the bucket decelerates together with the trapped electrons, yielding more energy in the form of radiation.

3.2 GINGER's Self-Design Taper Algorithm

The KMR formalism for tapered undulator is implemented in GINGER's self-design algorithm [9,10]. In the monochromatic, steady-state mode, this algorithm uses a special "design" macroparticle (kept at a specified beam radius r_d) and, by appropriately modifying the undulator parameter K at each z, maintains the macroparticle's ponderomotive phase $\psi_d \equiv \theta_d + \phi(r_d)$ at a specified value ψ_r according to Eqs. (3) and (5). The starting point of the taper is usually two gain lengths before saturation in order to prevent variations in $\phi(z)$ (associated with startup gain and diffraction effects) from affecting $K(z)$. For SASE that starts from shot noise, an effective input noise power is used in a monochromatic design run to determine the taper profile $K(z)$. With the resultant computed taper profile, the initial beam energy $\gamma_0 mc^2$ is then adjusted slightly to minimize the exponential gain length at the nominal

central wavelength of λ_r. This last adjustment is necessary because the peak gain generally occurs at a wavelength slightly longer than the resonant wavelength (corresponding to the design macroparticle) due to the energy spread and emittance effects.

There exists an optimal synchronous phase ψ_r for the best taper performance using the above algorithm. In the case of a monochromatic amplifier, since the bucket area (the area within the separatrix in the longitudinal phase space (η, ψ)) is approximately proportional to $\frac{1-\sin\psi_r}{1+\sin\psi_r}$ [11] and the bucket deceleration rate is proportional to $\sin\psi_r$ (see Eq. (5)), the average energy extraction rate is roughly proportional to the product of these two factors and is maximized at $\psi_r \approx 0.4$ rad [12]. In the case of SASE, the radiation field is spiky with the coherence length on the order of λ_r/ρ, a larger bucket area (i.e., at a smaller ψ_r) can help mitigate the electron detrapping due to the field inhomogeneity. In the following LEUTL and LCLS taper studies, we have found through extensive simulations that $\psi_r \approx 0.2$ rad appears to optimize the tapering performance in the SASE regime.

3.3 Tapered Undulator for LEUTL

The LEUTL FEL uses nine sections of 2.4-m undulator and has achieved saturation at $\lambda_r = 530$ nm and 385 nm between the sixth and the seventh sections [7]. Typical beam parameters are: rms bunch length of 0.3 ps, peak current of 266 A, normalized emittance $\gamma_0\varepsilon$ of 8.5 mm-mrad, and relative energy spread of 0.1% at 217 MeV. Using the self-design taper algorithm in GINGER, we have explored the tapering performance for the LEUTL FEL at 530 nm. After obtaining a smooth taper profile $K(z)$ with the optimal phase $\psi_r = 0.2$ rad, we take the average K value within each section for the un-

dulator sections 7, 8, and 9 to create a stepwise taper (i.e., $K = 3.09$, 3.07, 3.05, 3.02 for sections 1-6, 7, 8 and 9, respectively). This may be simpler to implement in practice than the continuous taper. As shown in Fig. 1, the average radiation energy at the end of the ninth undulator ($z = 21.6$ m) is slightly above 0.2 mJ for the tapered case, three times larger compared to the untapered case at the same z-location, and eight times larger compared to the nominal saturation level at the end of the sixth undulator. For the untapered case, the radiation energy slowly increases after saturation due to the sideband-like instability [2,13,14] but at the expense of increased spectral bandwidth. The average spectral power density will be proportional to the ratio of the average radiation energy to the relative rms bandwidth. This ratio is plotted in Fig. 2 and stays approximately constant after saturation in the untapered case as expected. Although the spectral bandwidth increases similarly due to the sidebands growth in tapered undulators [13], Fig. 2 clearly shows that tapering increases the average spectral power density by maintaining the resonant condition.

3.4 Tapered Undulator for LCLS

For the LCLS, we adopted relatively optimistic electron beam parameters (peak current of 3.4 kA, $\gamma_0\varepsilon = 1.0$ mm-mrad, $\sigma_\gamma/\gamma_0 = 7.1 \times 10^{-5}$ at 14.3 GeV) in order to examine the possibility of using a tapered undulator to enhance the energy efficiency. A 4.31-m-period FODO lattice provides the bulk of the focusing; no diagnostic drift sections are modeled in any of the following runs. With these beam parameters, GINGER SASE runs at $\lambda_r = 0.15$ nm show that power saturation occurs in an untapered undulator with 10 GW at $z \approx 60$ m with the power rising to 47 GW at $z = 200$ m. During this post-saturation

gain, the normalized rms spectral bandwidth increases from 4.8×10^{-4} to 1.4×10^{-3}. For comparison, the FEL scaling parameter $\rho = 5.3 \times 10^{-4}$.

Using the design strategy explained above, we had GINGER produce a taper profile $K(z)$ for $z \geq 35\,\mathrm{m}$ that decreased about 1.4% over the next 165 m. This taper does not take into account the additional energy loss due to the wideband spontaneous emission discussed in Sec. 2. Examination of Fig. 3 suggests that K drops nearly quadratically at first but then asymptotes to a nearly linear variation with z. As shown in Fig. 4, the average power of the tapered undulator SASE runs increases up to 174 GW by $z = 200\,\mathrm{m}$, about a factor of four over the untapered result at the same z-locations, and a factor of 17 in terms of energy efficiency over the saturation level. This power gain is nearly 50% of that predicted by the monochromatic tapered undulator run because of the significant detrapping associated with the poor temporal coherence of the SASE radiation field. Similar to the previous LEUTL studies, Fig. 5 shows the ratio of the average radiation power to the relative rms bandwidth for the SASE runs. The average spectral power density represented by this ratio stays almost constant after saturation for the untapered case but increases continuously for the tapered case.

4 Conclusions

We have discussed the use and the optimization of tapered undulators for SASE FELs in both the exponential growth regime and the saturation regime. Through numerical simulations using beam parameters based on the LEUTL and LCLS FELs, we have shown that tapering can be an effective method to increase the energy efficiency and the spectral power density for SASE FELs. The required change in the undulator parameter can be achieved by slightly

adjusting the undulator gap to change the undulator magnetic field. Additional work on tapering optimization and phase matching between undulator sections might further increase the attractiveness of using tapered undulators in SASE FELs.

We thank E. Moog, I. Vasserman, E. Saldin and M. Yurkov for useful discussions. Part of this work was supported by the U.S. Department of Energy under Contract Nos. W-31-109-ENG-38 and DE-AC03-76SF00098.

References

[1] R. Bonifacio, C. Pellegrini, and L.M. Narducci, Opt. Comm. **50**, 373 (1984).

[2] N.M. Kroll, P.L. Morton, and M.R. Rosenbluth, IEEE J. Quantum Electron., **QE-17**, 1436 (1981).

[3] Linac Coherent Light Source Design Study Report, SLAC-R-521, 1998.

[4] E. Gluskin *et al.*, Nucl. Instr. and Meth. A **429**, 358, (1999).

[5] M. Xie, Proceedings of the 1995 Particle Accelerator Conference, 183 (1995).

[6] N.A. Vinokurov, unpublished note.

[7] S. Milton *et al.*, Science **292**, 2037 (2001).

[8] N.A. Vinokurov, Nucl. Instr. and Meth. A **375**, 264, (1996). K.-J. Kim, M. Xie, C. Pellegrini, *ibid*, 314 (1996).

[9] T.J. Orzechowski, *et al.*, Phys. Rev. Lett. **57**, 2172 (1986).

[10] W.M. Fawley, CBP Tech Note-104, Lawrence Berkeley Laboratory, 1995.

[11] See, for example, S.Y. Lee, *Accelerator Physics* (World Scientific, Singapore, 1999).

[12] C.A. Brau and R.K. Cooper, in *Free-Electron Generators of Coherent Radiation*, Physics of Quantum Electronics **7**, 647 (1980).

[13] M.N. Rosenbluth, H.V. Wong and B.N. Moore, Phys. Fluids B **2**, 1635 (1990).

[14] R. Bonifacio *et al.*, Phys. Rev. Lett. **73**, 70 (1994).

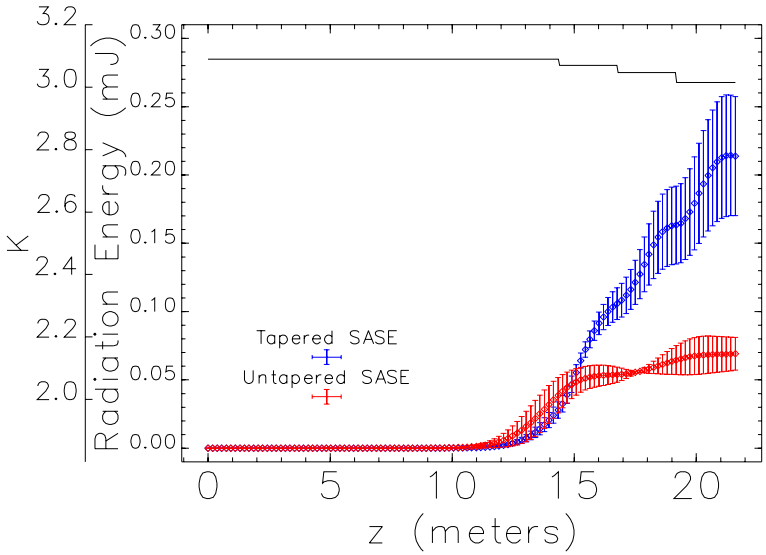

Fig. 1. The taper profile $K(z)$ used in the LEUTL simulations, the average and the statistical fluctuation of the radiation energy for the tapered and the untapered undulators.

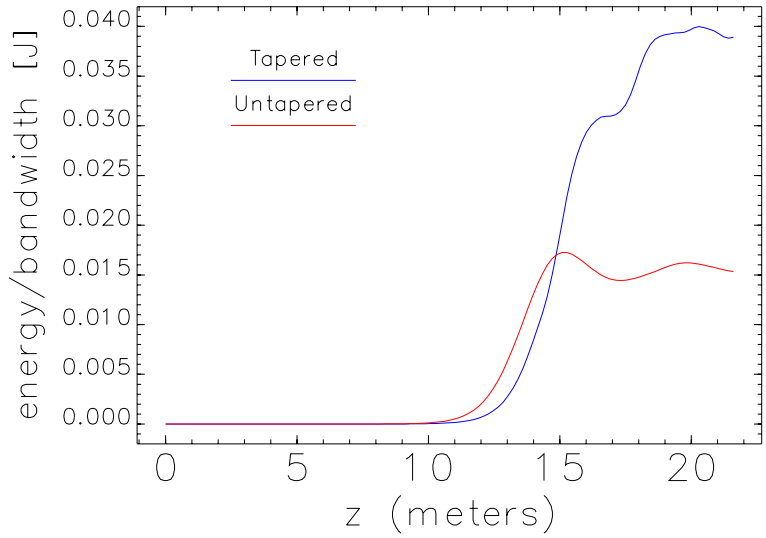

Fig. 2. The ratio of the average radiation energy to the relative rms bandwidth for the LEUTL untapered and tapered SASE simulations.

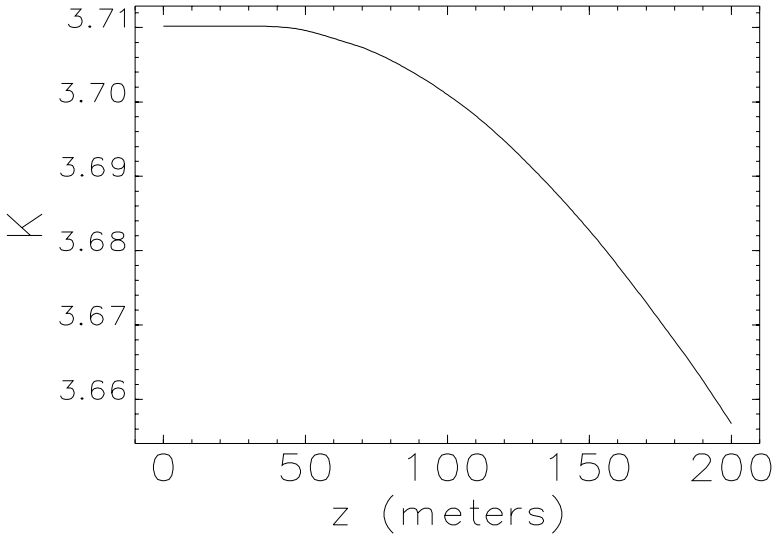

Fig. 3. GINGER-designed taper profile $K(z)$ for the LCLS.

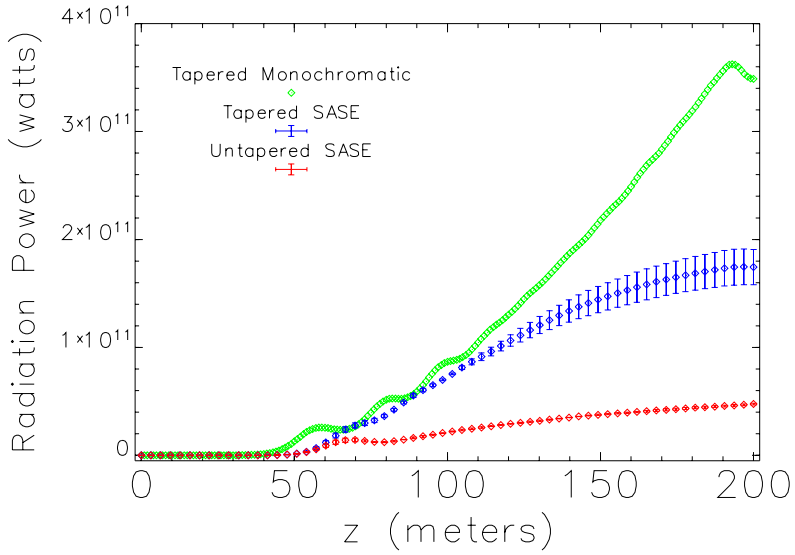

Fig. 4. Comparison of predicted power versus z for GINGER simulations of an untapered SASE run, tapered SASE runs, and tapered monochromatic amplifier run.

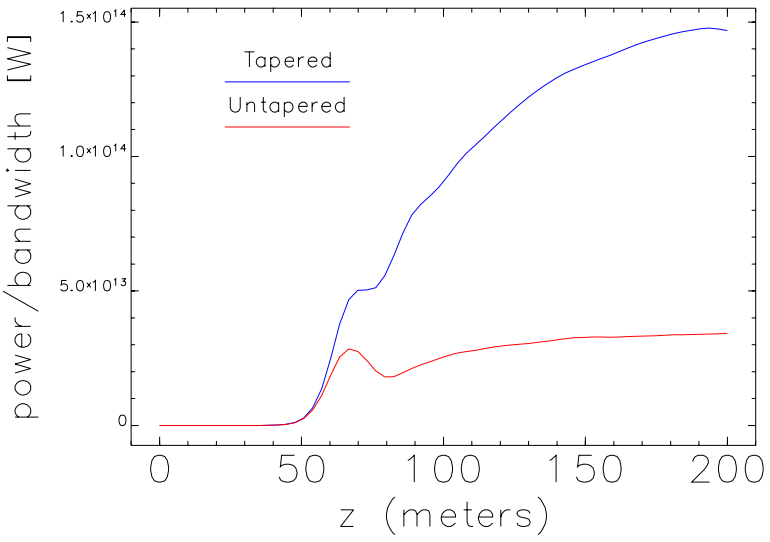

Fig. 5. The ratio of the average radiation power to the relative rms bandwidth for the LCLS untapered and tapered SASE simulations.